First passage time for a diffusive process under a geometric constraint

J. Stat. Mech. (2013) P09017

(http://iopscience.iop.org/1742-5468/2013/09/P09017)

Journal of Statistical Mechanics: Theory and Experiment
An IOP and SISSA journal

First passage time for a diffusive process under a geometric constraint

A A Tateishi[1,2], F S Michels[1], M A F dos Santos[1], E K Lenzi[1] and H V Ribeiro[1]

[1] Departamento de Física, Universidade Estadual de Maringá, Avenida Colombo, 5790-87020-900 Maringá-PR, Brazil
[2] Section for Science of Complex Systems, Medical University of Vienna, Spitalgasse 23, A-1090 Vienna, Austria
E-mail: aatateishi@dfi.uem.br, santanamichels@gmail.com, maikeafs@yahoo.com.br, eklenzi@dfi.uem.br and hvr@dfi.uem.br

Received 20 June 2013
Accepted 21 August 2013
Published 20 September 2013

Online at stacks.iop.org/JSTAT/2013/P09017
doi:10.1088/1742-5468/2013/09/P09017

Abstract. We investigate the solutions, survival probability, and first passage time for a two-dimensional diffusive process subjected to the geometric constraints of a backbone structure. We consider this process governed by a fractional Fokker–Planck equation by taking into account the boundary conditions $\rho(0,y;t) = \rho(\infty,y;t) = 0$, $\rho(x,\pm\infty;t) = 0$, and an arbitrary initial condition. Our results show an anomalous spreading and, consequently, a nonusual behavior for the survival probability and for the first passage time distribution that may be characterized by different regimes. In addition, depending on the choice of the parameters present in the fractional Fokker–Planck equation, the survival probability indicates that part of the system may be trapped in the branches of the backbone structure.

Keywords: exact results, stochastic particle dynamics (theory), diffusion

1742-5468/13/P09017+16$33.00

Contents

1. Introduction

Diffusion is one of the most important phenomena in nature, which depending on the situation can be usual [1] or anomalous [2]. The usual diffusion described, e.g., in terms of Langevin and Fokker–Planck equations [1] is connected to a Markovian process and has as main characteristic the mean square displacement (MSD) with a linear dependence on time, i.e., $\langle (r - \langle r \rangle)^2 \rangle \sim t$. The anomalous diffusion is characterized by a nonlinear behavior for the mean square displacement, $\langle (r - \langle r \rangle)^2 \rangle \propto t^{\alpha}$, with $\alpha \neq 1$ ($\alpha < 1$, $\alpha = 1$, and $\alpha > 1$ correspond to sub, normal, and superdiffusive processes, respectively). In general, anomalous diffusion has been investigated by using several approaches such as generalized Langevin equations [3], fractional [4]–[6] or nonlinear [7] Fokker–Planck equations, and continuous time random walks [8]. In the previous cases, as pointed out in [9, 10], knowledge of only the probability distribution function or the MSD may not be enough to provide all the information needed to understand the behavior of the system. In this sense, the survival probability and the first passage time (FPT) problem have been shown to be important tools to study and characterize the processes present in the systems that exhibit anomalous diffusive behavior. Typical examples include complex networks [11, 12], fractal structures [13, 14], animal foraging behavior [15]–[17], diffusion in membranes [18, 19], scale-invariant processes [20, 21], transport properties in biological cells [22]–[24], financial markets [25, 26], dynamics of cancer proliferation [27, 28], and reaction–diffusion kinetics [29, 30]. In particular, FTP analysis was used to distinguish the transport properties of two models of anomalous diffusion with the same probability distribution function in the long time limit [10], to compare the nonlinear diffusion equations of nonadditive entropies with the fractional diffusion model (once the Green functions of these equations leads to the exactly same MSD relation) [31] and as an unambiguous way to discriminate between microscopic models of subdiffusion [32].

Here, we investigate the solutions, survival probability, and the FPT distribution for a two-dimensional diffusive process subjected to the geometric constraint of a backbone structure (comb-model, see figure 1). This model was initially introduced to investigate anomalous diffusion in percolation clusters with topological bias [33, 34] wherein, according to [35], the backbone of the comb mimics the quasilinear structure of the cluster's backbone, and its branches assume the role of the dangling ends (or

J. Stat. Mech. (2013) P09017

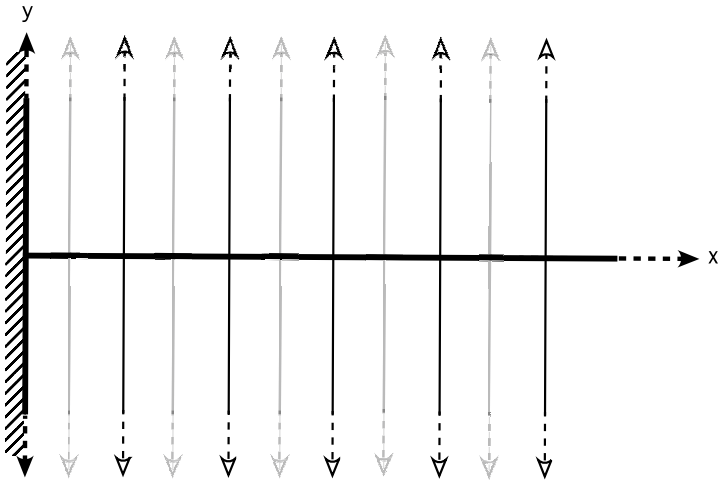

Figure 1. Illustration of the comb-model in a semi-infinite region. The x-direction represents the backbone structure, while the y-direction represents the branches. The hatched lines in $x = 0$ (hatched) correspond to the adsorbent surface.

trappings) of the percolation cluster. Then, a diffusive process subject to this structure is described by the following modified Fokker–Planck equation, as proposed in [36]:

$$\frac{\partial}{\partial t}\rho(x,y;t) = \mathcal{K}_y \frac{\partial^2}{\partial y^2}\rho(x,y;t) + \delta(y)\mathcal{K}_x \frac{\partial^2}{\partial x^2}\rho(x,y;t) \tag{1}$$

where $\mathcal{K}_y$ and $\mathcal{K}_x$ are diffusion coefficients in the x and y directions. The presence of the Dirac delta in equation (1) implies that the diffusion in the x-direction only occurs when $y = 0$. Consequently, the diffusion in the y-direction always occurs perpendicularly to the x-axis, thereby characterizing a comb-like structure. It is also interesting to mention that the effective probability distribution along the x-axis can be connected to the one obtained for a fractional diffusion equation with anomalous diffusion exponent 1/2 (see [36]). This result was generalized in [37], where a space–time fractional Fokker–Planck equation is derived from the comb-model.

As the intrinsic geometry of this model is a mechanism of anomalous diffusion, we can take advantage of this fact to consider in the same model other mechanisms that can lead to anomalous dynamical properties. For instance, in biological cells [38, 39], where the structure of intracellular environments is crowded and highly heterogeneous, the interactions among molecules and organelles are very complex producing different types of diffusion processes. In this sense, we analyze the following extension of equation (1):

$$\frac{\partial}{\partial t}\rho(x,y;t) = {}_0\mathcal{D}_t^{1-\gamma_y}\left(\mathcal{K}_y \frac{\partial^2}{\partial y^2}\rho(x,y;t)\right) + \delta(y)\ {}_0\mathcal{D}_t^{1-\gamma_x}\left(\mathcal{K}_x \frac{\partial^2}{\partial x^2}\rho(x,y;t)\right) \tag{2}$$

from which a rich class of diffusive processes can be obtained, where $\mathcal{K}_y$ and $\mathcal{K}_x$ are the diffusion coefficients and ${}_0\mathcal{D}_t^{1-\gamma_y}(\cdots)$ and ${}_0\mathcal{D}_t^{1-\gamma_x}(\cdots)$ are fractional time derivatives. In particular, we consider the Riemann–Liouville one [40], i.e.:

$${}_0\mathcal{D}_t^{1-\gamma}\left(\rho(x,y;t)\right) = \frac{1}{\Gamma(k-\gamma)}\frac{\mathrm{d}^k}{\mathrm{d}t^k}\int_0^t \mathrm{d}t'\,\frac{\rho(x,y;t')}{(t-t')^{\gamma-k+1}}, \tag{3}$$

with $k-1<\gamma<k$. Equation (2) extends equation (1) by incorporating fractional time derivatives that may be connected to several non-Markovian processes and, consequently, the ones worked out in [41]–[43]. In this case, we have considered different exponents of the time derivatives (γ_x and γ_y) in order to represent anisotropic systems where the kind of time correlations may depend strongly on the direction. In addition, fractional time derivatives have been recently applied to describe the anomalous diffusion in spiny dendrites [44, 45]. Similar to equation (1), the effective probability distribution which emerges from equation (2) along the x-axis can be connected to a fractional diffusion equation with anomalous diffusion exponent dependent on γ_x and γ_y. The boundary conditions used to investigate the solutions of equations (1) and (2) are $\rho(0,y;t)=\rho(\infty,y;t)=0$, and $\rho(x,\pm\infty;t)=0$, which are characterized by an adsorbent surface at $x=0$. We also consider an arbitrary initial condition $\rho(x,y;0)=\Phi(x,y)$, where $\Phi(x,y)$ is normalized.

This work is organized as follows. Section 2 is devoted to investigate the solutions, mean square displacement, survival probability, and FPT distribution obtained from equations (1) and (2). In section 3, we present our discussions and conclusions.

2. Survival probability and first passage time

Let us start our analysis by considering equation (1), which corresponds to a particular case of equation (2) for $\gamma_y=1$ and $\gamma_x=1$. Afterwards, we extend our discussion to equation (2) by taking $\gamma_y\neq 1$ and $\gamma_x\neq 1$ into account. This discussion is accomplished with the previous boundary and initial conditions. The solution for equation (1), subjected to the conditions previously mentioned, can be obtained by using integral transforms (Laplace and Fourier) and the Green function approach. In fact, applying the Laplace transform it is possible to show that

$$\mathcal{D}_y\frac{\partial^2}{\partial y^2}\rho(x,y;s)+\delta(y)\mathcal{D}_x\frac{\partial^2}{\partial x^2}\rho(x,y;s)=s\rho(x,y;s)-\Phi(x,y). \tag{4}$$

Equation (4), by using the Fourier transform, can be written as

$$\rho(x,y;s)=\frac{1}{\sqrt{4s\mathcal{K}_y}}\int_{-\infty}^{\infty}\Phi(x,\bar{y})\mathrm{e}^{-\sqrt{(s/\mathcal{K}_y)}|y-\bar{y}|}\,\mathrm{d}\bar{y}+\frac{\mathrm{e}^{-\sqrt{(s/\mathcal{K}_y)}|y|}}{\sqrt{4s\mathcal{K}_y}}\mathcal{D}_x\frac{\partial^2}{\partial x^2}\rho(x,0;s) \tag{5}$$

and, consequently, $y=0$ leads us to

$$\frac{\partial^2}{\partial x^2}\rho(x,0;s)-\frac{1}{\mathcal{K}_x}\sqrt{4s\mathcal{K}_y}\rho(x,0;s)=-\frac{1}{\mathcal{K}_x}\int_{-\infty}^{\infty}\Phi(x,\bar{y})\mathrm{e}^{-\sqrt{(s/\mathcal{K}_y)}|\bar{y}|}\,\mathrm{d}\bar{y}. \tag{6}$$

By using the Green function approach, the solution of equation (6) is given by

$$\rho(x,0;s)=-\int_0^{\infty}\mathrm{d}\bar{x}\int_{-\infty}^{\infty}\mathrm{d}\bar{y}\,\Phi(\bar{x},\bar{y})\mathrm{e}^{-\sqrt{(s/\mathcal{K}_y)}|\bar{y}|}\mathcal{G}_b(x,\bar{x};s), \tag{7}$$

where the Green function, $\mathcal{G}_b(x,\bar{x};s)$, is obtained from the following equation:

$$\frac{\partial^2}{\partial x^2}\mathcal{G}_b(x,\bar{x};s)-\frac{1}{\mathcal{K}_x}\sqrt{4s\mathcal{K}_y}\mathcal{G}_b(x,\bar{x};s)=\delta(x-\bar{x}) \tag{8}$$

J. Stat. Mech. (2013) P09017

subjected to the conditions $\mathcal{G}_b(0,\bar{x};s)=\mathcal{G}_b(\infty,\bar{x};s)=0$. Using the sin-Fourier and after performing some calculations, it is possible to show that equation (8) is satisfied by

$$\mathcal{G}_b(k_x,\bar{x};s)=-\sqrt{\frac{2}{\pi}}\frac{\sin\left(k_x\bar{x}\right)}{\sqrt{4\mathcal{K}_y s}/\mathcal{K}_x+k_x^2}\,. \tag{9}$$

Performing the inverse sin-Fourier transform in the previous equation, we obtain that the Green function, which governs the diffusive process in the x-axis, is given by

$$\mathcal{G}_b(x,\bar{x};s)=-\frac{1}{2}\sqrt{\frac{\mathcal{K}_x}{2\sqrt{\mathcal{K}_y s}}}\left(\mathrm{e}^{-\sqrt{(2/\mathcal{K}_x)\sqrt{\mathcal{K}_y s}}|x-x'|}-\mathrm{e}^{-\sqrt{(2/\mathcal{K}_x)\sqrt{\mathcal{K}_y s}}|x+x'|}\right) \tag{10}$$

and, consequently,

$$\begin{aligned}\rho(x,y;s)=&\frac{1}{\sqrt{4\mathcal{K}_y s}}\int_{-\infty}^{\infty}\mathrm{d}y'\,\Phi(x,y')\left(\mathrm{e}^{-\sqrt{(s/\mathcal{K}_y)}|y-y'|}-\mathrm{e}^{-\sqrt{(s/\mathcal{K}_y)}(|y|+|y'|)}\right)\\&-\frac{1}{\mathcal{K}_x}\int_0^{\infty}\mathrm{d}\bar{x}\int_{-\infty}^{\infty}\mathrm{d}\bar{y}\,\Phi(\bar{x},\bar{y})\mathrm{e}^{-\sqrt{(s/\mathcal{K}_y)}(|y|+|y'|)}\mathcal{G}_b(x,\bar{x};s).\end{aligned} \tag{11}$$

Note that the effective distribution which emerges in the Laplace space from equation (11) after performing an integration in the y variable corresponds to the one obtained for the one-dimensional fractional diffusion equation with the anomalous diffusion exponent $1/2$ for a system in a semi-infinity region for the initial condition $\Phi(x,y)=\bar{\Phi}(x)\delta(y)$. A similar situation for the effective distribution along the x direction has been verified in [36] for the boundary conditions $\rho(\pm\infty,y;t)=\rho(x,\pm\infty;t)=0$. It is also interesting to mention that using the solutions presented in [36] it is also possible to obtain the solution for equation (4) by employing the image method [46] when the previous initial condition is considered. Applying the inverse Laplace transform in equation (9), we obtain that

$$\begin{aligned}\mathcal{G}_b(x,\bar{x};t)=-\sqrt{\frac{\mathcal{K}_x}{8\sqrt{\mathcal{K}_y t^3}}}\Bigg\{&\mathrm{H}_{1,1}^{1,0}\left[\sqrt{\frac{2}{\mathcal{K}_x}}\sqrt{\frac{\mathcal{K}_y}{t}}|x-\bar{x}|\Big|_{(0,1)}^{(1/4,1/4)}\right]\\&-\mathrm{H}_{1,1}^{1,0}\left[\sqrt{\frac{2}{\mathcal{K}_x}}\sqrt{\frac{\mathcal{K}_y}{t}}|x+\bar{x}|\Big|_{(0,1)}^{(1/4,1/4)}\right]\Bigg\}\end{aligned} \tag{12}$$

and, consequently,

$$\rho(x,0;t)=-\int_0^{\infty}\mathrm{d}\bar{x}\int_{-\infty}^{\infty}\mathrm{d}\bar{y}\int_0^t\mathrm{d}\bar{t}\,\frac{|\bar{y}|}{\sqrt{4\pi\mathcal{K}_y\bar{t}^3}}\mathrm{e}^{-\bar{y}^2/4\mathcal{K}_y\bar{t}}\Phi(\bar{x},\bar{y})\mathcal{G}_b(x,\bar{x};t-\bar{t}) \tag{13}$$

(see the appendix for some details about the Fox H function). By using the previous results, the solution of equation (1) can be written as

$$\begin{aligned}\rho(x,y;t)=&\int_{-\infty}^{\infty}\mathrm{d}\bar{y}\,\Phi(x,\bar{y})(\mathcal{G}_u(|y-\bar{y}|;t)-\mathcal{G}_u(|y|+|\bar{y}|;t))\\&-\int_0^{\infty}\mathrm{d}\bar{x}\int_{-\infty}^{\infty}\mathrm{d}\bar{y}\int_0^t\mathrm{d}\bar{t}\,\frac{|y|+|\bar{y}|}{\sqrt{4\pi\mathcal{K}_y\bar{t}^3}}\mathrm{e}^{-(|y|+|\bar{y}|)^2/4\mathcal{K}_y\bar{t}}\Phi(\bar{x},\bar{y})\mathcal{G}_b(x,\bar{x};t-\bar{t})\end{aligned} \tag{14}$$

J. Stat. Mech. (2013) P09017

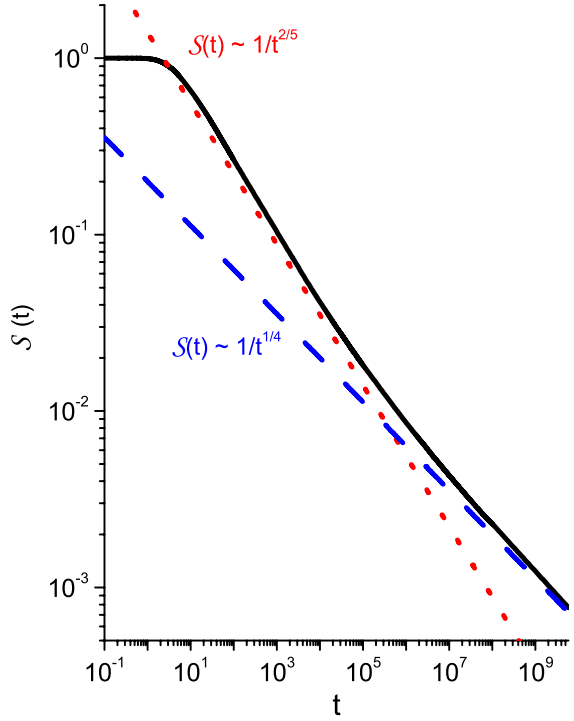

Figure 2. Behavior of equation (17) considering $\mathcal{K}_x = 10$, $\mathcal{K}_y = 0.1$, and the initial $\Phi(x, y) = \delta(x - \bar{x})\,\delta(y - \bar{y})$ with $\bar{x} = 1$ and $\bar{y} = 1.2$. The red and blue lines indicate the different regimes of the survival probability.

where $\mathcal{G}_u(y; t) = \mathrm{e}^{y^2/(4\mathcal{K}_y t)}/\sqrt{4\mathcal{K}_y t}$. Note that the presence of the first term in equation (14) depends on the initial condition and, in particular, it is absent for $\rho(x, y; 0) = \rho_x(x)\delta(y)$. Another interesting point connected with this term is the presence of different regimes in the survival probability and in the FPT distribution. As we will see below, this feature implies that, depending on the initial distribution of the system, it can present different behavior for these quantities due to the presence of different diffusive behavior manifested by the system, see figures 2 and 5. The MSD of the x-direction, $\sigma_x^2 = \langle (x - \langle x \rangle)^2 \rangle$, associated with equation (14), for $\Phi(x, y) = \delta(x - x')\delta(y - y')$, is given by

$$\sigma_x^2 = 2\mathcal{K}_x \sqrt{\frac{t}{\pi \mathcal{K}_y}}\,\mathrm{e}^{-y'^2/4\mathcal{K}_y t} - \frac{\mathcal{K}_x}{\sqrt{\mathcal{K}_y}} \int_0^t \mathrm{d}t' \, \frac{\mathrm{e}^{-y'^2/4\mathcal{K}_y (t-t')}}{\sqrt{\pi (t - t')}} \mathrm{H}_{1,1}^{1,0}\left[\sqrt{\frac{2}{\mathcal{K}_x}\sqrt{\frac{\mathcal{K}_y}{t'}}}\, x' \Big|_{(0,1)}^{(1,1/4)} \right]$$
$$+ x'^2 \int_0^t \mathrm{d}t' \, \frac{\mathrm{e}^{-y'^2/4\mathcal{K}_y (t-t')}}{\sqrt{\pi (t - t') t'}} \mathrm{H}_{1,1}^{1,0}\left[\sqrt{\frac{2}{\mathcal{K}_x}\sqrt{\frac{\mathcal{K}_y}{t'}}}\, x' \Big|_{(0,1)}^{(1/2,1/4)} \right]. \tag{15}$$

In the asymptotic limit of $t \to \infty$, the previous expression can be approximated to

$$\sigma_x^2 \sim \sqrt{\frac{2\mathcal{K}_x}{\sqrt{\mathcal{K}_y}}}\, x' \frac{t^{1/4}}{\Gamma(5/4)}. \tag{16}$$

Figure 3 illustrates the time behavior of equation (15). Note that the red line was incorporated to evidence the asymptotic diffusive regime which corresponds to

J. Stat. Mech. (2013) P09017

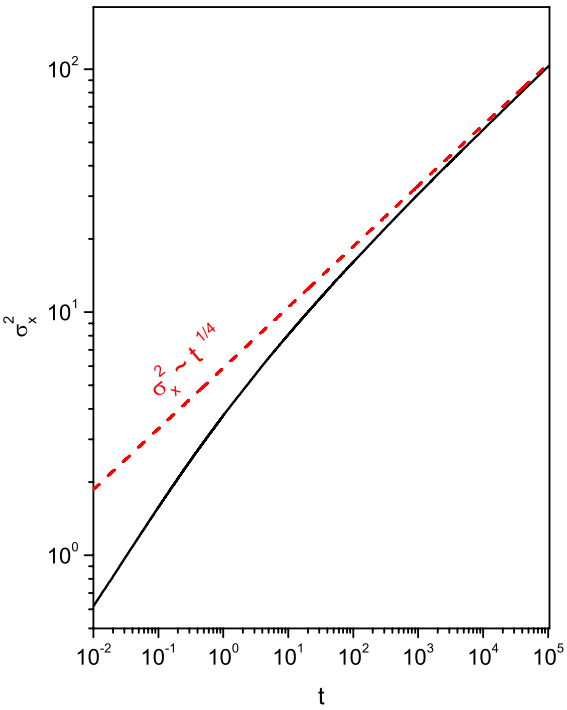

Figure 3. Behavior of the equation (15) considering $\mathcal{K}_x = 10$, $\mathcal{K}_y = 0.1$, and the initial $\Phi(x, y) = \delta(x - \bar{x})\,\delta(y)$ with $\bar{x} = 1.2$. The red line indicates the asymptotic regime.

equation (16). This anomalous exponent 1/4 can also be obtained for a three-dimensional comb model in the unlimited space [47]. However, in our case the anomalous exponent is less than in the usual two-dimensional comb due to the presence of an adsorbent surface. Now, we obtain the survival probability and the FPT distribution of the processes described by equation (14). Beyond the analytical solutions in terms of integral equations, we also show the algebraic tails (scaling laws) for the asymptotic time dependence by using the method reported in [48]. For the survival probability, i.e., $\mathcal{S}(t) = \int_0^\infty \mathrm{d}x \int_{-\infty}^\infty \mathrm{d}y\, \rho(x, y; t)$, we obtain that

$$\mathcal{S}(t) = \int_0^\infty \mathrm{d}x \int_{-\infty}^\infty \mathrm{d}y\, \Phi(x, y) \mathrm{erf}\left(\frac{|y|}{\sqrt{4\mathcal{K}_y t}}\right) + \int_0^\infty \mathrm{d}x \int_{-\infty}^\infty \mathrm{d}y\, |y| \Phi(x, y)$$
$$\times \int_0^t \frac{\mathrm{d}t'}{\sqrt{4\pi\mathcal{K}_y t'^3}} \mathrm{e}^{-y^2/4\mathcal{K}_y t'} \left\{1 - \mathrm{H}^{1,0}_{1,1}\left[\sqrt{\frac{2}{\mathcal{K}_x}\sqrt{\frac{\mathcal{K}_y}{t - t'}}}\, |x| \Big|^{(1,1/4)}_{(0,1)}\right]\right\}, \tag{17}$$

whose asymptotic behavior for long times is given by

$$\mathcal{S}(t) \sim \int_0^\infty \mathrm{d}x' \int_{-\infty}^\infty \mathrm{d}y'\, \Phi(x', y') \left(\left(\frac{|y'|}{\sqrt{\mathcal{K}_y}} - \frac{1}{\mathcal{K}_x}\sqrt{\mathcal{K}_y}\right)\frac{1}{\sqrt{\pi t}} + \sqrt{\frac{2}{\mathcal{K}_x}\sqrt{\mathcal{K}_y}}\frac{|x'|}{\Gamma(3/4)\, t^{1/4}}\right), \tag{18}$$

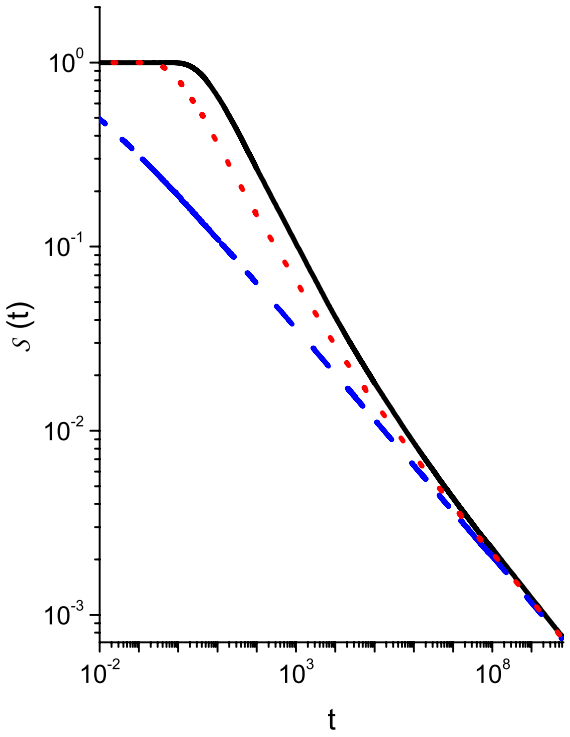

Figure 4. Behavior of equation (17) considering $\mathcal{K}_x = 10$, $\mathcal{K}_y = 0.1$, and the initial $\Phi(x, y) = \delta(x - \bar{x})\delta(y - \bar{y})$ with $\bar{x} = 1$ for different values of $\bar{y}$ in order to show the influence of the initial condition on the behavior of the survival probability. The blue, red, and black lines correspond to the cases $\bar{y} = 0$, $\bar{y} = 0.5$, and $\bar{y} = 1.2$.

and which, depending on the initial condition and the time scale considered, may be governed by the usual, $\mathcal{S}(t) \sim t^{-1/2}$, or the enhanced, $\mathcal{S}(t) \sim t^{-1/4}$, survival probability (first and second term present in equation (18), respectively) in the limit $t \to \infty$ with $|y'|/\sqrt{\mathcal{K}_y} > \sqrt{\mathcal{K}_y}/\mathcal{K}_x$. Figure 2 illustrates the behavior of equation (17) for values of $\mathcal{K}_x$, $\mathcal{K}_y$, $\bar{x}$, and $\bar{y}$. From this figure, we observe the presence of different diffusive regimes. One appears for short times and the other for long times as indicated by the (red and blue) lines present in figure 2. In particular, the long-time behavior corresponds to the second term in equation (18), since the first term for $t \to \infty$ has not a relevant contribution. The asymptotic behavior may also be obtained from the results presented in [36] by using the image method [46] to obtain the solution for the semi-infinity region or also by simple scaling arguments [49] once the model is related to the continuous time random walk along the x-direction with anomalous exponent 1/2. In figure 4, we illustrate the behavior of equation (17) for different choices of $\bar{y}$, which correspond to different positions for the initial condition. The results obtained by choosing different values of $\bar{y}$ show that the presence of different regimes depends on the choice of the initial condition. Moreover, a similar unusual asymptotic decay of the survival probability was reported in [50], where a velocity field (shear flow) is consider in the Fokker–Planck equation. However, in this work the result is obtained only due to the intrinsic geometrical constraints of the model.

The FPT may be obtained by using the definition $\mathcal{F}(t) = -\partial_t \mathcal{S}(t)$. After some calculations, it is possible to show that the FPT distribution connected to equation (17)

J. Stat. Mech. (2013) P09017

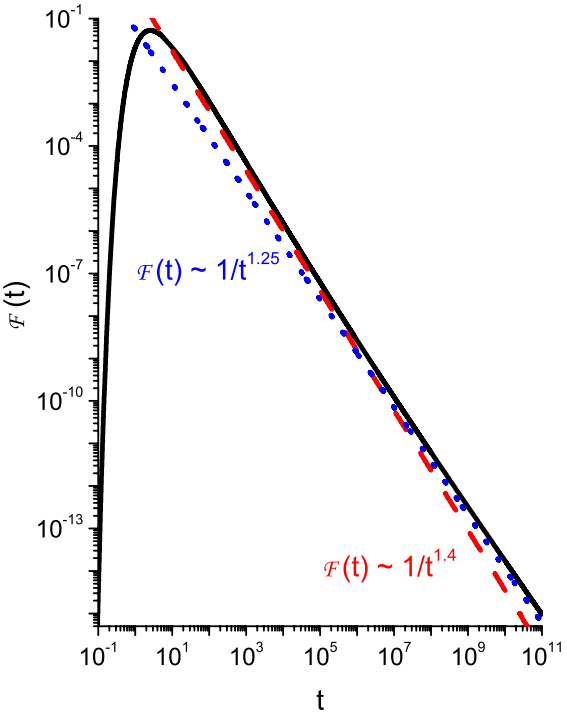

Figure 5. Behavior of equation (19) considering $\mathcal{K}_x = 10$, $\mathcal{K}_y = 0.1$, and the initial $\Phi(x, y) = \delta(x - \bar{x})\delta(y - \bar{y})$ with $\bar{x} = 1$ and $\bar{y} = 1.2$. The red and blue lines indicate the different regimes of the FPT distribution.

is given by

$$\mathcal{F}(t) = \int_0^\infty \mathrm{d}x \int_{-\infty}^\infty \mathrm{d}\bar{y}\, \Phi(x, y) \int_0^t \frac{\mathrm{d}\bar{t}}{\bar{t}} \frac{y\, \mathrm{e}^{-\bar{y}^2/4\mathcal{K}_y(t-\bar{t})}}{\sqrt{4\pi\mathcal{K}_y\,(t-\bar{t})^3}} \mathrm{H}_{1,1}^{1,0}\left[\sqrt{\frac{2}{\mathcal{D}_x}\sqrt{\frac{\mathcal{D}_y}{\bar{t}}}}\,|x|\Big|_{(0,1)}^{(1,1/4)}\right]. \tag{19}$$

The asymptotic behavior of the previous equation for long times is given by

$$\mathcal{F}(t) \sim \int_0^\infty \mathrm{d}x' \int_{-\infty}^\infty \mathrm{d}y'\, \Phi(x', y') \left(\left(\frac{|y'|}{\sqrt{\mathcal{K}_y}} - \frac{1}{\mathcal{K}_x}\sqrt{\mathcal{K}_y}\right)\frac{1}{2t\sqrt{\pi t}} + \sqrt{\frac{2}{\mathcal{K}_x}\sqrt{\mathcal{K}_y}}\frac{|x'|}{4\Gamma\,(3/4)\,t^{5/4}}\right). \tag{20}$$

Similar to the previous result obtained for the survival probability, depending on the initial condition the first or the second term may govern the asymptotic behavior of equation (20). In this sense, we can recover the results for the asymptotic behaviors of two different models of anomalous diffusion due to geometric constraints presented in [10]. The first one, $\mathcal{F}(t) \sim t^{-3/2}$, is related to the random walk and the second one, $\mathcal{F}(t) \sim t^{-5/4}$, is related to the comb model (continuous time random walk description). Figure 5 illustrates the behavior of equation (19) by considering, for simplicity, the values of $\mathcal{K}_x$ and $\mathcal{K}_y$ used in figure 2. Similarly to the results exhibited in figure 2, it presents two different regimes connected to the choice of the initial condition of the system. These results mean that

after an initial transient time some particles spend long periods trapped in the y-axis before being finally adsorbed in $x = 0$.

Now, we consider the general case where $\gamma_y \neq 1$ and $\gamma_x \neq 1$. In this manner, we are able to investigate how possible mechanisms of memory can affect the diffusive behavior in the backbone structure, i.e., we introduce memory effects connected to the fractional time derivatives present in equation (2). For this case, after some calculations, it is possible to show that the solution is given by

$$\begin{aligned}\rho(x,y;t) = &\int_{-\infty}^{\infty} \mathrm{d}\bar{y}\, \Phi(x,\bar{y}) \left(\bar{\mathcal{G}}_y\left(|y-\bar{y}|;t\right) - \bar{\mathcal{G}}_y\left(|y|+|\bar{y}|;t\right)\right) \\ &+ \int_0^{\infty} \mathrm{d}\bar{x} \int_{-\infty}^{\infty} \mathrm{d}\bar{y} \int_0^t \mathrm{d}\bar{t}\, \Phi(\bar{x},\bar{y}) \\ &\times \mathcal{G}_y\left(|y|+|\bar{y}|;t-\bar{t}\right) \left(\mathcal{G}_b\left(|x-\bar{x}|;\bar{t}\right) - \mathcal{G}_b\left(|x+\bar{x}|;\bar{t}\right)\right) \end{aligned} \tag{21}$$

with

$$\bar{\mathcal{G}}_y(y;t) = \frac{1}{\sqrt{4\mathcal{K}_y t^{\gamma_y}}} \mathrm{H}_{1,1}^{1,0}\left[\frac{|y-\bar{y}|}{\sqrt{\mathcal{K}_y t^{\gamma_y}}}\middle|_{(0,1)}^{(1-\gamma_y/2,\gamma_y/2)}\right], \tag{22}$$

$$\mathcal{G}_y(y;t) = \frac{1}{t\sqrt{4\mathcal{K}_y/t^{\gamma_y}}} \mathrm{H}_{1,1}^{1,0}\left[\frac{|y|+|\bar{y}|}{\sqrt{\mathcal{K}_y \bar{t}^{\gamma}}}\middle|_{(0,1)}^{(1-\gamma_y/2,\gamma_y/2)}\right], \tag{23}$$

and

$$\begin{aligned}\mathcal{G}_b(x;t) = \sqrt{\frac{2\sqrt{\mathcal{K}_y t^{\gamma_y}}}{\mathcal{K}_x t^{2\gamma_x}}} \Bigg(&\mathrm{H}_{1,1}^{1,0}\left[\sqrt{\frac{2\sqrt{\mathcal{K}_y t^{\gamma_y}}}{\mathcal{K}_x t^{\gamma_x}}}\,|x|\,\middle|_{(0,1)}^{(1-(1/2)(\gamma_x-\gamma_y/2),(1/2)(\gamma_x-\gamma_y/2))}\right] \\ &- \mathrm{H}_{1,1}^{1,0}\left[\sqrt{\frac{2\sqrt{\mathcal{K}_y t^{\gamma_y}}}{\mathcal{K}_x t^{\gamma_x}}}\,|x|\,\middle|_{(0,1)}^{(1-(1/2)(\gamma_x-\gamma_y/2),(1/2)(\gamma_x-\gamma_y/2))}\right]\Bigg). \end{aligned} \tag{24}$$

Similar to the previous case, the MSD for the processes connected to equation (21) with $\Phi(x,y) = \delta(x-x')\delta(y-y')$ is given by

$$\begin{aligned}\sigma_x^2 = &\frac{\mathcal{K}_x}{\sqrt{\mathcal{K}_y}} t^{\eta} \mathrm{H}_{1,1}^{1,0}\left[\sqrt{\frac{2}{\mathcal{K}_x t^{\gamma_x}}\sqrt{\mathcal{K}_y t^{\gamma_y}}}\,x'\,\middle|_{(0,1)}^{(1+\eta,\gamma_y/2)}\right] \\ &- \frac{\mathcal{K}_x}{\sqrt{\mathcal{K}_y}} \int_0^t \frac{\mathrm{d}t'}{t'^{1-\eta}} \mathrm{H}_{1,1}^{1,0}\left[\frac{|y'|}{\sqrt{\mathcal{K}_y (t-t')^{\gamma_y}}}\middle|_{(0,1)}^{(1,\gamma_y/2)}\right] \\ &\times \mathrm{H}_{1,1}^{1,0}\left[\sqrt{\frac{2}{\mathcal{K}_x t'^{\gamma_x}}\sqrt{\mathcal{K}_y t'^{\gamma_y}}}\,x'\,\middle|_{(0,1)}^{(1+\eta,\eta/2)}\right] \\ &+ x'^2 \int_0^t \frac{\mathrm{d}t'}{t'} \mathrm{H}_{1,1}^{1,0}\left[\frac{|y'|}{\sqrt{\mathcal{K}_y (t-t')^{\gamma_y}}}\middle|_{(0,1)}^{(1,\gamma_y/2)}\right] \\ &\times \mathrm{H}_{1,1}^{1,0}\left[\sqrt{\frac{2}{\mathcal{K}_x t'^{\gamma_x}}\sqrt{\mathcal{K}_y t'^{\gamma_y}}}\,x'\,\middle|_{(0,1)}^{(0,\eta/2)}\right], \end{aligned} \tag{25}$$

J. Stat. Mech. (2013) P09017

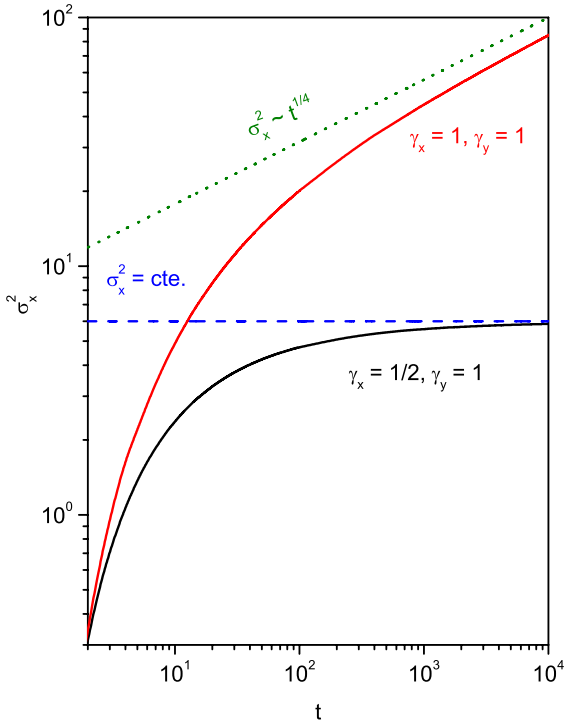

Figure 6. Behavior of the equation (25) considering $\mathcal{K}_x = 10$, $\mathcal{K}_y = 0.1$, and the initial $\Phi(x, y) = \delta(x - \bar{x})\,\delta(y - \bar{y})$ with $\bar{x} = 1$ and $\bar{y} = 1.2$. The blue and green straight lines were incorporated in this figure to indicate the asymptotic behaviors of the variance.

where $\eta = \gamma_x - \gamma_y/2$. In the asymptotic limit of $t \to \infty$, we obtain that

$$\sigma_x^2 \sim \sqrt{\frac{2\mathcal{K}_x}{\sqrt{\mathcal{K}_y}}} \frac{t^{\eta/2}}{\Gamma(1 + \eta/2)}. \tag{26}$$

For this case the asymptotic time dependence is characterized by both anomalous exponents γ_x and γ_y. Note that the presence of memory effects in the branches and in the backbone can lead to the slower diffusion in the system. In figure 6 is illustrated the time behavior of equation (25) for values of γ_x and γ_y. An interesting point is the presence of a stationary situation for the σ_x^2 depending on the choice of γ_x and γ_y. Stationary behaviors (saturation plateau) and subdiffusion with the MSD scaling exponent around 1/4 can be related to the confined motion and the molecular crowding, as has been reported in single-particle tracking experiments in living cells [51, 52]. Particularly, the authors in [53] show that these anomalous relaxation dynamics are influenced by combined effects of the molecular crowding (due the presence of worm-like micelles) and the optical traps (optical tweezer setup). In fact, these nontrivial features of the interplay between memory effects and geometric constraints also appear in the survival probability and the FPT distribution connected to the process described by equation (21). Therefore, by using the previous

J. Stat. Mech. (2013) P09017

definitions, these transport properties are given by

$$\mathcal{S}(t) = 1 - \int_0^\infty \mathrm{d}x \int_{-\infty}^\infty \mathrm{d}y \int_0^t \mathrm{d}t' \, \frac{\Phi(x,y)}{\sqrt{t'(t-t')}} \mathrm{H}_{1,1}^{1,0}\left[\frac{|y|}{\sqrt{\mathcal{K}_y \left(t-t'\right)^{\gamma_y}}} \middle|_{(0,1)}^{(0,\gamma_y/2)} \right] \times \mathrm{H}_{1,1}^{1,0}\left[\sqrt{\frac{2\sqrt{\mathcal{K}_y t'^{\gamma_y}}}{\mathcal{K}_x t'^{\gamma_x}}} \, |x| \middle|_{(0,1)}^{(0,1/2(\gamma_x-\gamma_y/2))} \right] \tag{27}$$

and

$$\mathcal{F}(t) = \int_0^\infty \mathrm{d}x \int_{-\infty}^\infty \mathrm{d}y \int_0^t \mathrm{d}t' \, \frac{\Phi(x,y)}{t'(t-t')} \mathrm{H}_{1,1}^{1,0}\left[\frac{|y|}{\sqrt{\mathcal{K}_y \left(t-t'\right)^{\gamma_y}}} \middle|_{(0,1)}^{(0,\gamma_y/2)} \right] \times \mathrm{H}_{1,1}^{1,0}\left[\sqrt{\frac{2\sqrt{\mathcal{K}_y t'^{\gamma_y}}}{\mathcal{K}_x t'^{\gamma_x}}} \, |x| \middle|_{(0,1)}^{(0,1/2(\gamma_x-\gamma_y/2))} \right]. \tag{28}$$

For equations (27) and (28), the asymptotic behavior for long times is governed by

$$\mathcal{S}(t) \sim \frac{1}{\Gamma\left(1-\eta/2\right) t^{\eta/2}} \sqrt{\frac{2}{\mathcal{K}_x}\sqrt{\mathcal{K}_y}} \int_0^\infty \mathrm{d}x' \int_{-\infty}^\infty \mathrm{d}y' \, |x'| \Phi(x',y') \tag{29}$$

and

$$\mathcal{F}(t) \sim \frac{\eta}{2t^{1+\eta/2}\Gamma\left(1-\eta/2\right)} \sqrt{\frac{2}{\mathcal{K}_x}\sqrt{\mathcal{K}_y}} \int_0^\infty \mathrm{d}x' \int_{-\infty}^\infty \mathrm{d}y' \, |x'| \Phi(x',y'). \tag{30}$$

In figure 7 we illustrate the behavior of the survival probability of equation (27) for the case $\gamma_x = \gamma_y/2$ with $\gamma_y = 1$ and $\gamma_x = \gamma_y = 1$. For the first case, we verify that the behavior of $\mathcal{S}(t)$ in the asymptotic limit of long times is a constant, in contrast to the second case. This feature suggests that the memory effects can enhance the survival probability, i.e., part of the system remains trapped in the branches and, consequently, is not absorbed by the surface present in $x = 0$. The asymptotic behavior is governed by $\mathcal{S}(t) \sim 1/t^{\eta/2}$ and is influenced also by temporal correlations in the branches, which are represented by the exponent γ_y. This fact together with the results of equation (19) suggest that for this model a nontrivial behavior of the survival probability due to memory effects can appear independently on the choices of initial condition and time scale, whereas the effects geometrical constraints may be neglected depending on these choices. The same analysis can be applied for the FPT given by equation (28).

3. Discussion and conclusions

We have investigated the solution, MSD, survival probability, and the FPT distribution of the diffusive processes connected to equation (2), where a backbone structure and fractional time derivatives are present. These quantities were obtained by considering the system in a semi-infinity region in the x-direction with an adsorbent boundary condition in $x = 0$ for an arbitrary initial condition. Even for the simplest case, $\gamma_x = \gamma_y = 1$, nontrivial results are obtained due to the geometrical constraints. Depending on the initial condition, the system may exhibit different diffusive regimes: one for small times and the other for

J. Stat. Mech. (2013) P09017

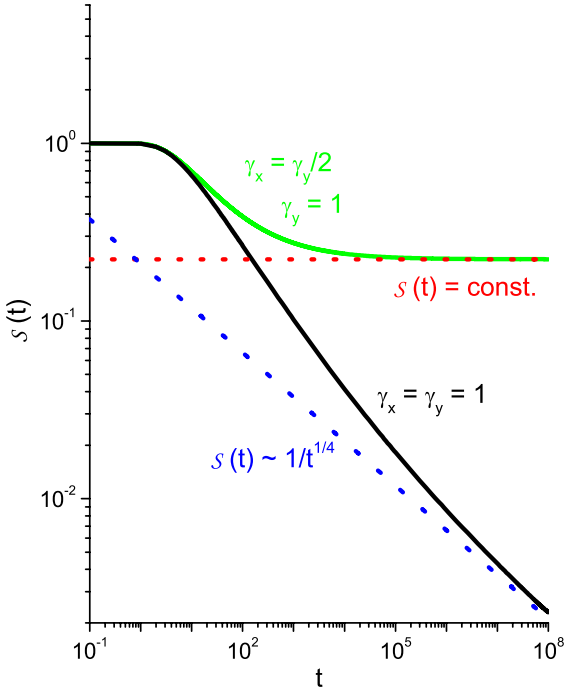

Figure 7. Behavior of the equation (29) considering $\mathcal{K}_x = 10$, $\mathcal{K}_y = 0.1$, and the initial $\Phi(x, y) = \delta(x - \bar{x})\,\delta(y - \bar{y})$ with $\bar{x} = 1$ and $\bar{y} = 1.2$ in order to show the influence of the initial condition on the behavior of the survival probability. The blue and red lines correspond to the asymptotic behavior of the survival probability for long times.

long times, as indicated in figures 2 and 5 by the straight lines (blue and red). In this sense, figure 4 shows that one of these regimes connected to the initial condition may not be manifested. After, we have added memory effects by considering the general case $\gamma_x \neq 1$ and $\gamma_y \neq 1$ where we showed that, depending on the choice of γ_x and γ_y, particles can remain trapped in the branches of the backbone structure and consequently not be absorbed by the surface present in $x = 0$. This feature is illustrated in figures 6 and 7 for $\gamma_x = \gamma_y/2$, which leads us to a constant value for $\sigma_x^2(t)$ and $\mathcal{S}(t)$ in the asymptotic behavior of long times. From these figures we also observe that the MSD increases with the same scaling exponent as for the survival probability decrease. This means that the presence of memory effects can slow down the diffusive motion in the x-direction, consequently enhancing the survival probability. Moreover, our results also suggest that the choices of the initial condition and the time scale play important roles in the detection of the anomalous dynamics due to geometrical constraints and memory effects. Finally, we hope that the results presented here may be useful in the discussion of the systems where the backbone structure and anomalous diffusion are present, and in the study of memory effects in diffusive systems with traps.

Acknowledgments

We would like to thank to CNPq and CAPES (Brazilian agencies) for partial financial support. In particular, AAT is grateful to CAPES for the support under grant number

1502-12-5 and HVR is grateful to CAPES/Fundação Araucária for financial support under grant number 113/2013.

Appendix. Fox H function

The Fox H function (or H-function) may be defined in terms of the Mellin–Branes type integral [54, 55]

$$\begin{aligned} \mathrm{H}_{p,q}^{m,n}\left[x|_{(b_q,B_q)}^{(a_p,A_p)}\right] &= \mathrm{H}_{p,q}^{m,n}\left[x|_{(b_1,B_1),\ldots,(b_q,B_q)}^{(a_1,A_1),\ldots,(a_p,A_p)}\right] = \frac{1}{2\pi \mathrm{i}}\int_L \chi(\xi)x^{-\xi}\,\mathrm{d}\xi \\ \chi(\xi) &= \frac{\Pi_{j=1}^{m}\Gamma\left(b_j - B_j\xi\right)\Pi_{j=1}^{n}\Gamma\left(1-a_j+A_j\xi\right)}{\Pi_{j=m+1}^{q}\Gamma\left(1-b_j+B_j\xi\right)\Pi_{j=n+1}^{p}\Gamma\left(a_j-A_j\xi\right)}, \end{aligned} \tag{A.1}$$

where m, n, p and q are integers satisfying $0 \le n \le p$ and $1 \le m \le q$. It may also be defined by its Mellin transform

$$\int_0^\infty \mathrm{H}_{p,q}^{m,n}\left[ax|_{(b_q,B_q)}^{(a_p,A_p)}\right] x^{\xi-1}\,\mathrm{d}x = a^{-\xi}\chi(\xi). \tag{A.2}$$

Here, the parameters have to be defined such that $A_j > 0$ and $B_j > 0$ and $a_j(b_h+\nu) \neq B_h(a_j-\lambda-1)$ where $\nu, \lambda = 0, 1, 2, \ldots, h = 1, 2, \ldots, m$ and $j = 1, 2, \ldots, m$. The contour L separates the poles of $\Gamma\left(b_j - B_j\xi\right)$ for $j = 1, 2, \ldots, m$ from those of $\Gamma\left(1-a_j+A_j\xi\right)$ for $j = 1, 2, \ldots, n$ [54]. The H-function is analytic in x if either (i) $x \neq 0$ and $M > 0$ or (ii) $0 < |x| < 1/B$ and $M = 0$, where $M = \sum_{j=1}^{q} B_j - \sum_{j=1}^{p} A_j$ and $B = \prod_{j=1}^{p} A_j^{A_j}\prod_{j=1}^{q} B_j^{-B_j}$. Some useful properties of the Fox H function found in [54] are listed below.

(i) The H-function is symmetric in the pairs $(a_1, A_1), \ldots, (a_p, A_p)$, likewise $(a_{n+1}, A_{n+1}), \ldots, (a_p, A_p)$; in $(b_1, B_1), \ldots, (b_q, B_q)$ and in $(b_{n+1}, B_{n+1}), \ldots, (b_q, B_q)$.

(ii) For $k > 0$

$$\mathrm{H}_{p,q}^{m,n}\left[x|_{(b_q,B_q)}^{(a_p,A_p)}\right] = k\mathrm{H}_{p\,q}^{m\,n}\left[x^k|_{(b_q,kB_q)}^{(a_p,kA_p)}\right]. \tag{A.3}$$

(iii) The multiplication rule is

$$x^k\mathrm{H}_{p,q}^{m,n}\left[x|_{(b_q,B_q)}^{(a_p,A_p)}\right] = \mathrm{H}_{p,q}^{m,n}\left[x|_{(b_q+kB_q,B_q)}^{(a_p+kA_p,A_p)}\right]. \tag{A.4}$$

(iv) For $n \ge 1$ and $q > m$,

$$\mathrm{H}_{p,q}^{m,n}\left[x|_{(b_1,B_1)\cdots(b_{q-1},B_{q-1})(a_1,A_1)}^{(a_1,A_1)(a_2,A_2)\cdots(a_p,A_p)}\right] = \mathrm{H}_{p-1,q-1}^{m,n-1}\left[x|_{(b_1,B_1)\cdots(b_{q-1},B_{q-1})}^{(a_2,A_2)\cdots(a_p,A_p)}\right]. \tag{A.5}$$

(v) For $m \ge 2$ and $p > n$

$$\mathrm{H}_{p,q}^{m,n}\left[x|_{(b_1,B_1)(b_2,B_2)\cdots(b_q,B_q)}^{(a_1,A_1)\cdots(a_{p-1},A_{p-1})(b_1,B_1)}\right] = \mathrm{H}_{p-1,q-1}^{m-1,n}\left[x|_{(b_2,B_2)\cdots(b_q,B_q)}^{(a_2,A_2)\cdots(a_{p-1},A_{p-1})}\right]. \tag{A.6}$$

(vi) The relation between the generalized Mittag-Leffler function and the Fox H function is given by

$$\mathrm{E}_{\alpha,\beta}(x) = \mathrm{H}_{1,2}^{1,1}\left[-x|_{(0,1)(1-\beta,\alpha)}^{(0,1)}\right]. \tag{A.7}$$

J. Stat. Mech. (2013) P09017

(vii) Under Fourier cosine transformation, the H-function transforms as

$$\int_0^\infty \mathrm{H}_{p,q}^{m,n}\left[k\middle|\begin{matrix}(a_p,A_p)\\(b_q,B_q)\end{matrix}\right]\cos(kx)\,\mathrm{d}x=\frac{\pi}{x}\mathrm{H}_{q+1,p+2}^{n+1,m}\left[x\middle|\begin{matrix}(1-b_q,B_q),(1,1/2)\\(1,1),(1-a_p,A_p),(1,1/2)\end{matrix}\right]. \tag{A.8}$$

References

[1] Gardiner C W, 1996 *Handbook of Stochastic Methods: For Physics, Chemistry and the Natural Sciences* (*Springer Series in Synergetics*) (New York: Springer)
[2] Pekalski A and Sznajd-Weron K (ed), 1999 *Anomalous Diffusion: From Basics to Applications* (*Springer Lecture Notes in Physics*) (Berlin: Springer)
[3] Muralidhar R, Ramkrishna D, Nakanishi H and Jacobs D, 1990 *Physica* A **167** 539
[4] Metzler R and Klafter J, 2000 *Phys. Rep.* **339** 1
[5] Hilfer R, Metzler R, Blumen A and Klafter J (ed) 2002 *Strange kinetics*, *Chem. Phys.* **284** 1
[6] Klafter J, Lim S C and Metzler R (ed), 2011 *Fractional Dynamics: Recent Advances* (Singapore: World Scientific)
[7] Frank T D, 2005 *Nonlinear Fokker–Planck Equations: Fundamentals and Applications* (Heidelberg: Springer)
[8] Weiss G H, 1994 *Aspects and Applications of the Random Walk* (Amsterdam: North-Holland)
[9] Dybiec B and Gudowska-Nowaki E, 2009 *Phys. Rev.* E **80** 061122
[10] Meroz Y, Sokolov I M and Klafter J, 2011 *Phys. Rev. Lett.* **107** 260601
[11] Zhang Z, Yang Y and Lin Y, 2012 *Phys. Rev.* E **85** 011106
[12] Meyer B, Agliari E, Bnichou O and Voituriez R, 2012 *Phys. Rev.* E **85** 026113
[13] Meroz Y, Sokolov I M and Klafter J, 2011 *Phys. Rev.* E **83** 020104(R)
[14] Lin Y, Wu B and Zhang Z, 2010 *Phys. Rev.* E **82** 031140
[15] Fauchald P and Tveraa T, 2003 *Ecology* **84** 282
[16] Bailleul F, Pinaud D, Hindell M, Charrassin J-B and Guinet C, 2008 *J. Anim. Ecol.* **77** 5
[17] Byrne M E and Chamberlain M J, 2012 *Anim. Behav.* **84** 593
[18] van Hijkoop V J, Dammers A J, Malek K and Coppens M-O, 2007 *J. Chem. Phys.* **127** 085101
[19] Wei F, Yang D, Straube R and Shuai J, 2011 *Phys. Rev.* E **83** 021919
[20] Condamin S, Bnichou O, Tejedor V, Voituriez R and Klafter J, 2007 *Nature* **450** 77
[21] Carretero-Campos C, Bernaola-Galvn P, Ivanov P Ch and Carpena P, 2012 *Phys. Rev.* E **85** 011139
[22] Lua R C and Grosberg A Y, 2005 *Phys. Rev.* E **72** 061918
[23] Lagache T and Holcman D, 2008 *Phys. Rev.* E **77** 030901(R)
[24] Kenwright D A, Harrison A W, Waigh T A, Woodman P G and Allan V J, 2012 *Phys. Rev.* E **86** 031910
[25] Perell J, Gutierrez-Roig M and Masoliver J, 2011 *Phys. Rev.* E **84** 066110
[26] Masoliver J and Perell J, 2009 *Phys. Rev.* E **80** 016108
[27] Iomin A, 2006 *Phys. Rev.* E **73** 061918
[28] Iomin A, 2005 *J. Phys.: Conf. Ser.* **7** 57
[29] Bénichou O, Chevalier C, Klafter J, Meyer B and Voituriez R, 2010 *Nature Chem.* **2** 472
[30] Loverdo C, Bnichou O, Moreau M and Voituriez R, 2008 *Nature Phys.* **4** 134
[31] Kosztolowicz T and Lewandowska K D, 2012 *Phys. Rev.* E **86** 021108
[32] Condamin S, Tejedor V, Voituriez R, Bénichou O and Klafter J, 2008 *Proc. Nat. Acad. Sci.* **105** 5675
[33] White S R and Barma M, 1984 *J. Phys. A: Math. Gen.* **17** 2995
[34] Bunde A, Havlin S, Stanley H E, Trus B and Weiss G H, 1986 *Phys. Rev.* B **34** 8129
[35] ben-Avraham D and Havlin S, 2000 *Diffusion and Reactions in Fractals and Disordered Systems* (Cambridge: Cambridge University Press)
[36] Arkhincheev V E and Baskin E M, 1991 *Zh. Eksp. Teor. Fiz.* **100** 292 [1991 *Sov. Phys.—JETP* **73** 161]
[37] Elwakil S A, Zahran M A and Abulwafa E M, 2004 *Chaos Solitons Fractals* **20** 1113
[38] Höfling F and Franosch T, 2013 *Rep. Prog. Phys.* **76** 046602
[39] Regner B M *et al,* 2013 *Biophys. J.* **104** 1652
[40] Podlubny I, 1999 *Fractional Differential Equations* (San Diego, CA: Academic)
[41] Arkhincheev V E, 2000 *Physica* A **280** 304
[42] Arkhincheev V E, 2010 *Physica* A **389** 1
[43] Tateishi A A, Lenzi E K, Ribeiro H V, Evangelista L R, Mendes R S and da Silva L R, 2011 *J. Stat. Mech.* P02022
[44] Méndez V and Iomin A, 2013 *Chaos Solitons Fractals* **53** 46
[45] Iomin A and Méndez V, 2013 *Phys. Rev.* E **88** 012706

J. Stat. Mech. (2013) P09017

[46] Wyld H W, 1999 *Mathematical Methods for Physics* (Boulder, CO: Perseus Books)
[47] Arkhincheev V E, 1999 *JETP* **88** 710
[48] Krapivsky P L, Redner S and Ben-Naim E, 2010 *A Kinetic View of Statistical Physics* (Cambridge: Cambridge University Press)
[49] Bray A J, Majumdar S N and Schehr G, 2013 *Adv. Phys.* **62** 225
[50] Redner S and Krapivsky P L, 1996 *J. Stat. Phys.* **82** 999
[51] Jeon J-H and Metzler R, 2012 *Phys. Rev.* E **85** 021147
[52] Leijnse N, Jeon J-H, Loft S, Metzler R and Oddershede L B, 2012 *Eur. Phys. J. Spec. Top.* **204** 75
[53] Jeon J-H, Leijnse N, Oddershede L B and Metzler R, 2013 *New J. Phys.* **15** 045011
[54] Mathai A M, Saxena R K and Haubold H J, 2009 *The H-Function: Theory and Applications* (New York: Springer)
[55] Metzler R and Nonnenmacher T F, 2002 *Chem. Phys.* **284** 67